

Pericellular Matrix Enhances Retention and Cellular Uptake of Nanoparticles

Rui Zhou, Haiying Zhou, Bin Xiong, Yan He,* and Edward S. Yeung

State Key Laboratory of Chemo/Biosensing and Chemometrics, College of Chemistry and Chemical Engineering, College of Biology, Hunan University, Changsha 410082, P.R. China.

Supporting Information

ABSTRACT: A hydrated gel-like pericellular matrix (PCM) covers the surface of all eukaryotic cells and plays a key role in many cellular events, but its effect on nanoparticle internalization has not been studied. Here, using cells with various PCM thicknesses and gold nanoparticles as probes, we demonstrate that, rather than being a barrier to all foreign objects, the PCM can entrap and accumulate NPs, restrict and slow down their diffusion, and enhance their cellular uptake efficiency. Moreover, this newly discovered PCM function consumes energy and seems to be an integral part of the receptor-mediated endocytosis process. These findings are important in understanding the delivery mechanisms of nanocarriers for biomedical applications.

INTRODUCTION

Nanoparticles (NPs) with unique physical and chemical properties have been extensively exploited as drug carriers and gene delivery agents into cells for targeted or controlled therapeutic and biomedical imaging applications.^{1–5} The potential cytotoxicity of NPs is also of increasing public concern.^{6,7} Continuous advancements in these areas require a deep understanding of interactions between cells and NPs, especially the cellular uptake of NPs. So far, many reports have shown that NP properties, such as size, shape, and surface modification, can influence how they are internalized by cells.^{8,9} The impact of sedimentation of large and heavy NPs,¹⁰ the protein corona bound to NP surface,¹¹ and the role of cell cycle have also been studied.¹² However, detailed operations of the cellular machinery that leads to NP entering cells as efficiently as virus particles are still not well understood. An implied assumption in almost all previous studies is that the first contact between an invading NP and the cell occurs at the plasma membrane (PM), which is perceived as the outmost physical boundary between the intracellular and extracellular environment. Thus, researches have been concentrated on specific or nonspecific interactions between NPs and the phospholipid bilayer and the embedded proteins or protein networks.¹³ In reality, the PM is not exposed directly to the exterior solution but is surrounded by a hydrated gel-like network of membrane-bound polysaccharides and glycoproteins. This cell coating is usually a few micrometers thick and is referred to as the glycocalyx or the pericellular matrix (PCM).¹⁴ The PCM, being the true interaction zone between a cell and its external environment, participates in the transportation of ions, molecules and particles across the PM and plays a key role in the motion, proliferation, differentiation, and apoptosis of many cell types.^{15,16} As far as NP internalization is concerned, the role of the PCM has largely been ignored or is merely regarded as a passive barrier to NPs.¹⁷ Herein, by using plasmonic imaging and single-particle analysis techniques, we demonstrate that the PCM can play an active role by trapping and accumulating NPs, resulting in an enhanced cellular NP

internalization efficiency. Therefore, many earlier works may need to be re-evaluated to account for the effect of the PCM.

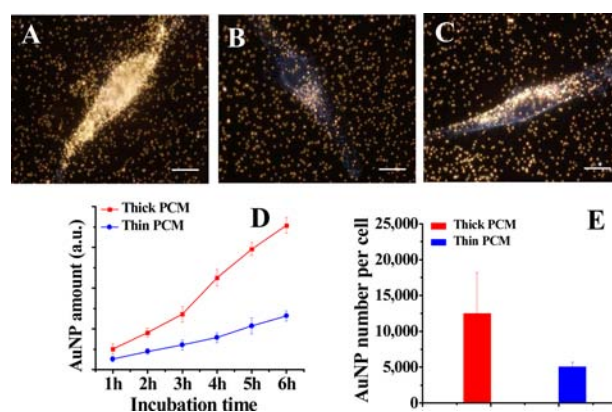


Figure 1. Typical dark field microscopy (DFM) images of (A) AuNP retention by a thick-PCM cell, (B) AuNP acquisition by a thin-PCM cell, and (C) AuNP internalization by a thick-PCM cell after its PCM layer and the associated AuNPs are removed. (D) Semiquantitative comparison of AuNPs internalized by thick- and thin-PCM cells after various AuNP incubation times. (E) Quantitative comparison of AuNP uptake by a thick- or thin-PCM cell using inductively coupled plasma atomic emission spectroscopy (ICP-AES). The scale bar is 20 μ m. The AuNP incubation time is 4 h for A, B, C, and E.

RESULTS AND DISCUSSION

In our studies, MG-63, a human osteosarcoma cell line having a thick PCM layer¹⁸ was used as the model cell. It is well-known that one major component of the PCM is hyaluronan (HA), which is a polysaccharide that serves as the mechanical scaffold for the assembly of other cell-secreted molecules such as glycoproteins to form a cell-associated network structure. After

Received: May 6, 2012

Published: August 3, 2012

the cells are treated with hyaluronidase (HA'ase), the HA molecules and the scaffold are degraded, and the PCM collapses effectively,¹⁹ but the biological activity of a cell is still maintained.^{20,21} So the HA'ase-treated MG-63 cells can serve as the control cell with a thin PCM layer. The PCM thickness difference between the normal MG-63 cells (thick-PCM cells) and the HA'ase-treated ones (thin-PCM cells) can be visualized clearly from the particle sedimentation assay (Figure S1, Supporting Information [SI]), which provides the boundary of the PCM extension on the substrate.²² Note that since the cells produce HAs and other PCM components continuously, the PCM layer can never be depleted completely. We used a carboxylic acid (mercaptosuccinic acid, MSA) terminated, negatively charged, gold nanoparticles (AuNPs) of 90–120 nm in size as probes because AuNPs are photostable, biocompatible, and easy to prepare and modify chemically and biologically.²³ Single AuNPs larger than 80 nm produce very strong plasmonic scattering emission under oblique illumination of white light and are readily distinguishable (yellow) from the intracellular scattering background (white) under a dark field microscope (DFM).²⁴ Additional assays indicate that these AuNPs are monodisperse, do not aggregate in the cell culture medium that contains serum, and have almost no cytotoxicity (Figure S2, SI).

Figure 1A and Figure 1B show the DFM images after incubating 120-nm AuNPs with thick-PCM cells and thin-PCM cells for 4 h, respectively. It can be seen that the thick-PCM cell accumulates a large amount of AuNPs that form excessive aggregates and generate intense scattering emission. In contrast, there are fewer AuNPs accumulated by the thin-PCM cell, and they appear as weaker discrete spots. To identify the AuNPs that are truly internalized by the cells without interference from those being trapped in the PCM, we removed the PCM and the associated AuNPs from the thick-PCM cell surface by using HA'ase after the 4-h cell/NP incubation (Figure 1C). The image shows that the cells with a thick PCM have a higher AuNP uptake efficiency than those with a thin PCM. Further comparison of DFM images (Figure S3, SI) and the image analysis results (Figure 1D) after culturing the cells with AuNPs for various amounts of time demonstrated that the thick-PCM cells acquired many more AuNPs than the thin-PCM cells. To quantify the average number of AuNPs internalized by the two types of cells, we collected the cells after 4 h incubation with 120-nm AuNPs via trypsinization (which also disrupted the PCM and released the PCM-trapped AuNPs outside the PM) and performed inductively coupled plasma atomic emission spectroscopy (ICP-AES) analysis on the dissolved cells. Figure 1E shows that, on average, a cell with a thick PCM internalized about 12,500 AuNPs, and a thin-PCM cell internalized about 5000 AuNPs. Taken together, our data suggest that the PCM significantly enhanced the cellular uptake efficiency of AuNPs by first accumulating a high concentration of AuNPs in the PCM and then allowing more particles to enter the cell.

To better reveal the accumulation of particles in the PCM, we incubated the cells with 90-nm AuNPs for 4 h and stained them using FM 1-43, a fluorescent dye that only binds to lipid molecules and can mark the boundary of the PM. At the same time we obtained optical sections (slice thickness \sim 700 nm) of AuNP scattering and FM 1-43 fluorescence of the cells with a laser scanning confocal microscope (LSCM). Figure 2A and Figure 2B show the LSCM images sliced at the middle of a thick-PCM cell and a thin-PCM cell, respectively. More z-sectioning results are displayed in Figure S4, SI. Evidently, the

cell with thick PCM has a wide pericellular zone concentrated with AuNPs outside the PM, but few AuNPs can be observed beyond the cell membrane of the thin-PCM cell. By keeping the optical focal plane of the LSCM at the PCM region of a normal MG-63 cell, the AuNP trapping process was recorded in real time (Figure S5, SI). It can be seen that after adding AuNPs into the cell culture medium, the distribution of AuNPs was initially random across the field of view. With increasing time the regions around the cells accumulated more and more particles, while the concentration of AuNPs in other regions remained almost constant. After about 60 min, continuous trapping of particles made the shapes of the cells gradually visible, indicating the local concentration of AuNPs was significantly higher than other places in the cell culture medium. Since higher NP concentration in the cell culture medium usually leads to more NPs entering the cell,²⁵ the enhanced AuNP uptake efficiency should be a direct consequence of trapping and accumulating AuNPs by the PCM, which allows more AuNPs to interact with the PM.

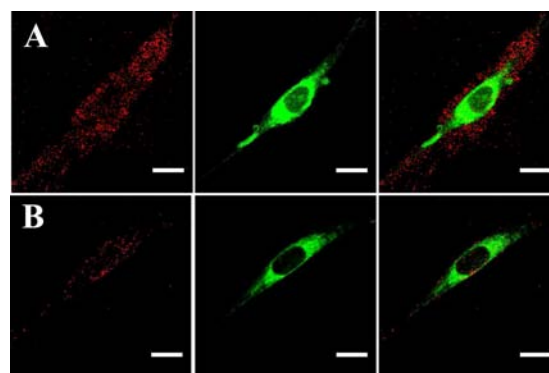


Figure 2. Confocal images of AuNP scattering (left), FM 1-43 fluorescence that marks the PM boundary (middle), and their overlay (right) for a thick-PCM cell (A) and a thin-PCM cell (B) after incubating them with AuNPs for 4 h. The scale bar is 20 μ m.

To find out if the same phenomenon occurs in other cell lines with a less abundant PCM, we performed similar experiments on HeLa cells whose PCM thickness is close to that of the HA'ase-treated MG-63 cells (Figure S1, SI). Figure S6 (SI) and Figure 3 show the typical cellular images and AuNP counting results after culturing normal, HA'ase-treated and ascorbic acid (AA)-pretreated HeLa cells with 120-nm AuNPs for 1 h, respectively. It has been reported by others that adding AA into the cell growth medium repeatedly for 3 days could enhance the density and viscosity of the PCM.²² Compared with the average 98 ± 11 AuNP uptake by one normal HeLa cell, depleting the PCM by using HA'ase leads to less AuNP uptake (58 ± 10) and enhancing the PCM by adding AA leads to more AuNP uptake (171 ± 17), although the differences are not as dramatic as in the case of MG-63 cells. Therefore, the ability of the PCM to enhance NP internalization seems to be ubiquitous. It should be noted that because the PCM of HeLa cells is relatively thin, it is hard to experimentally differentiate the AuNPs trapped in PCM from those internalized. That is probably the reason why the PCM effect was not noticed previously.

Generally, the PCM has been considered as the protective layer to shield the cell against mechanical and chemical damage and to keep foreign particles and molecules away from the cell surface.¹⁹ It has been reported that the PCM can reduce the

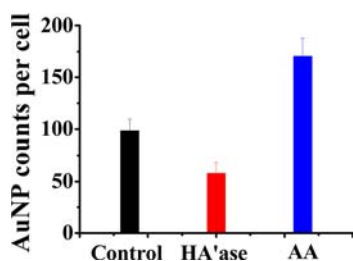


Figure 3. Number of AuNPs internalized by one cell after incubating 120-nm AuNPs with normal HeLa cells, HA'ase-treated HeLa cells, and ascorbic acid-pretreated HeLa cells for 1 h, respectively. Fifty cells from five replicate experiments were counted in each case.

ability of small molecules such as DNA^{18,26} and sodium ions²⁷ to penetrate into cells. Thus, it is surprising that the PCM can recruit AuNPs and assist their cellular internalization. One possibility is that the observed PCM effect is caused by the precipitation of the AuNPs, since 120-nm AuNPs are heavy and tend to settle to the bottom of the cell culture dish within 12 h. Thus, we incubated normal and HA'ase-treated MG-63 cells with 50-nm AuNPs that are light and well dispersed in the cell medium within at least 36 h. A similar PCM trapping effect was observed (Figure S7, SI). Therefore, the AuNP accumulation is not induced by gravity, and some structural properties of the PCM that favor their uptake must be involved.

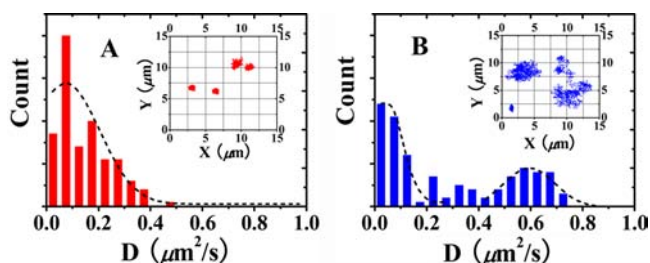


Figure 4. Distribution of 120-nm AuNP diffusion coefficients measured near the cell surface of thick-PCM (A) and thin-PCM (B) cells. The inserts are the corresponding typical trajectories.

According to previous studies, our AuNPs should be covered by serum proteins from the culture medium due to nonspecific absorption and enter into cells via receptor-mediated endocytosis (RME) pathway.²⁵ Dynamic light scattering and ζ potential measurements on the AuNPs (Table S1, SI) show a significant size increase and charge reduction of the highly negatively charged particles after they are added into the cell medium, indicating that serum proteins strongly adsorbed onto the AuNP surface. On the other hand, the PCM is characterized by a network structure with increased viscosity and combined negative and positive charge patches.^{17,28} So the answer must lie in the relationship between the kinetic behaviors of membrane receptors and the motions of AuNPs within the gel-like network structure of the PCM. For this purpose, we performed single particle tracking (SPT) analysis on the diffusion behaviors of individual AuNPs near the PM surface of both normal MG-63 cells with a thick PCM and HA'ase-treated cells with a thin PCM (Figure 4). It can be seen that in both situations the diffusion coefficients of most AuNPs are less than $0.8 \mu\text{m}^2/\text{s}$, which is considerably smaller than the value in the culture medium ($\sim 2.0 \mu\text{m}^2/\text{s}$) but much larger than those on the cell membrane ($< 0.01 \mu\text{m}^2/\text{s}$). This is consistent with our

previous study that the motion of AuNPs is slowed down in the pericellular environment regardless the PCM thickness.²⁹ Comparing the two, however, the motions of all AuNPs observed in the thick PCM are restricted in small compartments of $1\text{--}3 \mu\text{m}$ and the distribution of their diffusion coefficient, D , has only one population centered at $0.07 \mu\text{m}^2/\text{s}$. In contrast, the trajectories of AuNPs obtained from the thin-PCM cells display two populations: one is also confined in tight regions with the D distribution centered at $0.04 \mu\text{m}^2/\text{s}$; the other is more close to free motion with the D distribution centered at $0.59 \mu\text{m}^2/\text{s}$. Since thick-PCM cells can internalize more AuNPs, the SPT results imply that the diffusion rate of AuNPs near the cell surface could affect their cellular uptake. To test this argument, we varied the viscosity of the cell-growth medium by adding different amounts of HA (MW $\approx 10,000$) and used them to culture thin-PCM cells together with AuNPs for 4 h. Figure S8 (SI) indicates that a higher viscosity of the medium or a slower AuNP diffusion rate did lead to more particles entering the cell.

It is well-known that RME is a complex cellular process that is composed of multistep coordination of many molecules and molecular assemblies on and near the PM.^{30,31} When one receptor is activated, intracellular signal transductions lead to recruitment of other membrane proteins or expression of specific genes. A ubiquitous phenomenon is that a ligand-binding event will trigger receptors diffusing to the binding site and receptors clustering to sustain the internalization process. In the case of small molecules, usually just one receptor is needed to capture a molecular ligand to initiate its RME process. Due to their tiny size and fast diffusion rate, a free space without a viscous PCM above the PM would allow a ligand to sample large areas of the PM with little steric hindrance or electrostatic repulsion and to find and bind to the appropriate receptor quickly. The situation would be similar to that where the molecule needs no receptor to enter the cell. Thus, the cellular uptake efficiency of small molecules is enhanced if the PCM is thin or removed.^{18,26} However, a protein-coated AuNP is a huge multivalent ligand with a large inertia. It is likely that a significant number of membrane receptors and related molecules would have to redistribute to its adjacency, rearrange around it, and aggregate together to bind to the surface of the AuNP before it can be brought into the cell. All these courses of action require a certain amount of time and could be facilitated if the AuNP is restricted in a limited space with a slow diffusion rate compared to that of nearby receptors. Previous studies have shown that the diffusion coefficient of a protein receptor during its clustering process is $\sim 0.1 \mu\text{m}^2/\text{s}$,^{32,33} which is very close to the measured $0.07 \mu\text{m}^2/\text{s}$ value of AuNPs confined in the compartmentalized thick PCM layer. Hence, the PCM could act as a buffering zone to provide more time for the recruitment and clustering of receptors and allow effective interaction between the receptors and the trapped AuNPs. Preliminary results from similar SPT measurements on 90- and 50-nm AuNPs indicate that the thick PCM layer can bring the diffusion coefficient of different AuNPs all down to about $0.1 \mu\text{m}^2/\text{s}$ regardless of their size (data not shown). In addition, a thick, 3D, gel-like structure could accommodate more AuNPs, effectively raising their concentration adjacent to the cell membrane. On the other hand, cells with thin or no PCM have a relatively smooth membrane surface. With no obstacles from the PCM scaffold, individual AuNPs in the solution may not be readily captured by approaching just one anchoring point on the PM because of

their large momentum. As a result, it is reasonable to observe two types of particle motions due to the inhomogeneous distribution of membrane receptors. In one case, the AuNP may hit and stick to a large cluster of receptors by chance, exhibiting a much restricted trajectory with a very slow diffusion rate ($0.04 \mu\text{m}^2/\text{s}$). In the other case, the AuNP diffuses randomly on top of the PM swiftly ($0.59 \mu\text{m}^2/\text{s}$), probably keeps breaking loose from attachments to a few receptors, and cannot stay at one location long enough to permit efficient binding with sufficient numbers of receptors or the formation of receptor clusters. The effective concentration of the AuNPs is also lower without the help of the PCM. These factors all lead to less efficient AuNP uptake. Indeed with thin-PCM cells, many AuNPs were observed approaching the PM from the solution, bouncing on it several times and finally escaping back into the solution (Movie S1). But with thick-PCM cells, almost all AuNPs near the PM stayed in their own compartment. Although occasionally an AuNP jumping from one compartment to another occurred, no trapped particles were observed leaving the PCM to return to the bulk solution (Movie S2). Our finding thus provides another viewpoint on why NP-based drug carriers have higher delivery efficiency than the small-molecule drugs alone.³⁴

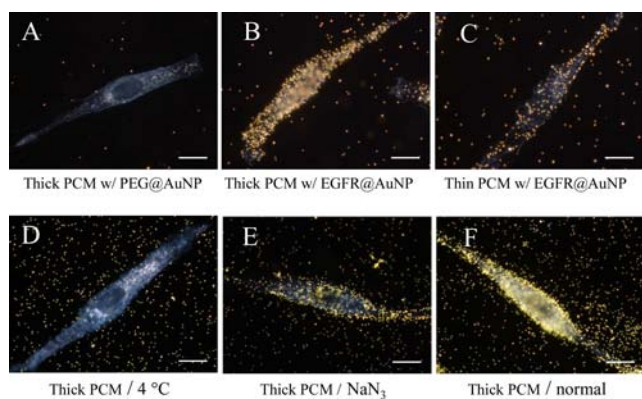


Figure 5. (A–C) Cellular uptake of PEG (A) and anti-EGFR (B, C)-coated 120-nm AuNPs after incubating with thick-PCM cells (A, B) and thin-PCM cells (C) for 1 h. (D–F) Cellular uptake of AuNPs at 4 °C (D), at 37 °C after NaN_3 treatment (E), and at 37 °C (F) after incubating unmodified 90-nm AuNPs with thick-PCM cells for 2 h. The scale bar is 20 μm .

Therefore, according to the SPT analysis, the 3D gel-like network structure of the PCM may provide a buffering zone to entrap and slow down AuNPs, and allow AuNP–receptor complexes to form efficiently. One question remaining is whether the PCM operates independently with a relatively static structure or it functions as a dynamic and integral part of RME. To answer this question, we first tested if the PCM has some selectivity toward AuNPs with certain surface chemistry. We modified AuNPs with poly(ethylene glycol) (PEG) and anti-epidermal growth factor receptor (anti-EGFR), respectively, and cultured them together with both normal and HA₂ase-treated MG-63 cells. It is well-known that PEG-coated particles have little affinity toward proteins and resist cellular uptake *in vitro*,³⁵ and EGFR is an overexpressed membrane receptor in most tumor cells.³⁶ From DFM results, no PEG-modified AuNP trapping by the PCM was observed (Figure 5A), but the accumulation behaviors of anti-EGFR-coated AuNPs by the thick- and thin-PCM cells were almost the same

as those of serum protein-coated AuNPs (Figure 5B and Figure 5C). Thus, the PCM does not grab AuNPs without discrimination, and at least a certain degree of protein coverage is needed before the AuNPs can pass its screening. Further investigations on the selectivity of the PCM toward other specific protein coatings and surface modifications are underway. Second, we tested whether the accumulation of AuNPs in the PCM is energy dependent like RME.³⁷ Figure 5D shows that, at 4 °C, AuNPs were neither internalized by the cell nor trapped by the PCM. Similarly, if cellular ATP was depleted by adding sodium azide, PCM trapping of AuNPs was also much reduced (Figure 5E). Hence, PCM accumulation of AuNPs also consumes energy and is synchronized with RME. Taken together, the above results suggest that structural organization of the PCM network is changing dynamically and is regulated by RME. In this regard, the PCM behave more like an active functional extension layer of the PM than a passive gel-like cover over the cell. We note that this active role of PCM may not have been discovered if purified components had been utilized to construct the PCM-like hydrogel.^{17,38,39} More studies are being performed to elucidate this phenomenon.

CONCLUSIONS

In conclusion, with plasmonic imaging and a model cell with thick- vs thin-PCM, we have demonstrated that the PCM can play a significant role during the NP internalization process. Rather than being a barrier to the transport of all foreign objects, the PCM can entrap and accumulate certain types of NPs and enhance their cellular uptake efficiency. Moreover, this newly discovered PCM function seems to be an integral part of the complex receptor-mediated endocytosis (RME) mechanism. For a long time it was believed that the only way for a cell to form receptor clusters around a ligand entering the cell, thereby speeding up its cellular uptake, was to form a special membrane-bound compartment that concentrates those receptors.⁴⁰ Only during recent years did researchers come to recognize that cells can utilize scaffold protein-based sub-compartments that are not membrane-enclosed for the same purpose.⁴¹ Now our findings point out that the smart cellular machinery may also make use of the pericellular matrix to form large compartments to facilitate its internalization of NPs. Hence, targeting the PCM components and structure, especially for cells (e.g., stem cells) with abundant PCM, could be a new route to modulate the cellular uptake of NPs loaded with drugs or genes. This viewpoint is fundamentally important in understanding the RME process and the delivery mechanisms of NP-based carriers for biomedical applications.

MATERIALS AND METHODS

Chemicals. HAuCl_4 , sodium citrate, 2-mercaptosuccinic acid (MSA), paraformaldehyde, Na_2HPO_4 , NaCl , NaH_2PO_4 were purchased from Sinopharm Chemical (Shanghai, China). Anti-EGFR, thiolated poly(ethylene glycol) (PEG-SH, MW \approx 5,000), 1-ethyl-3-[3-(dimethylamino)propyl] (EDC), *N*-hydroxysulfosuccinimide (Sulfo-NHS) were obtained from Sigma-Aldrich (U.S.A.).

AuNP Preparation and Characterization. MSA-modified AuNPs were synthesized using a seed-mediated method.⁴² Briefly, 1.03 mL of 2.428×10^{-2} M HAuCl_4 was gently mixed with 98.97 mL DI water (Millipore, 18.2 M Ω) and then heated to boil for 5 min. Then 0.588 mL of 0.2 M sodium citrate solution was rapidly injected into the boiling solution. The mixture was vigorously stirred and refluxed for 30 min. After the color of the mixture was changed to wine red, the colloidal solution was kept stirring at room temperature for another 15 min and then was filtered through a 0.22 μm filter. The

seed AuNPs prepared by this protocol have an average size of about 18 nm. To prepare MSA-modified 120-, 90-, and 50-nm AuNPs, 0.070, 0.120, and 0.500 mL of 18-nm AuNP seeds, respectively, 0.165 mL of 2.428×10^{-2} M HAuCl_4 , and 0.24 mL of 0.01 M MSA were added into 20 mL of DI-water sequentially. The growth process lasted for 2 h. The size of the resulting AuNPs was determined using TEM. The hydrodynamic radius and surface charge of the AuNPs were obtained using a Malvern Nano ZS instrument.

Surface Modification of AuNPs. For AuNP modification using anti-EGFR antibody, 1.0 mL of as-prepared MSA-modified AuNP solution was centrifuged twice at 6000 rpm and resuspended in 1.0 mL of MES buffer (pH = 5.5). 100 μL of 0.4 M EDC and 100 μL of 0.1 M Sulfo-NHS were then added into the solution. The mixture was sonicated at room temperature for about 1 h, washed via centrifugation twice, and redispersed in phosphate buffer (pH = 7.4). 50 μL of 182.5 mM Anti-EGFR solution was then added into the AuNP solution, and sonicated for another 1.5 h. The mixture was centrifuged and redispersed in phosphate buffer (pH = 7.4). For PEG-SH modification of AuNPs, 1.0 mL of as-prepared AuNPs were concentrated to 500 μL via centrifugation. Then 500 μL of 1.0 mM PEG-SH solution was added. After shaking for 2 h, the AuNPs were collected by centrifugation and redispersed in water.

Cell Culture. Cervical cancer HeLa cells and osteosarcoma MG-63 cells were obtained from American Type Culture Collection (ATCC). The cells were cultured on a coverglass placed in a plastic culture dish and maintained in high DMEM (Dulbecco's Modified Eagle's medium with high glucose, GIBCO) supplemented with 10% fetal bovine serum (GIBCO) at 37 °C and 5% CO_2 in a humidified atmosphere.

Cell Viability Assay. MG-63 cell and HeLa cells were both seeded in 96-well plates at 1×10^3 cells/well in medium supplemented with 10% fetal bovine serum. After 24 h incubation, cells were washed with PBS (Hyclone) and then exposed to a medium containing AuNPs with various concentrations. After another 24 h incubation, cell viability was measured by the standard MTT assay.

Particle Exclusion Assay. Human erythrocytes were donated by a volunteer in our lab. They were centrifuged at 2000 rpm for 5 min, washed extensively with PBS, and then fixed with 4% formaldehyde for 2 h. After being washed three times using PBS, the fixed erythrocytes were resuspended in PBS with 0.1% BSA. To identify the pericellular region of MG-63 or HeLa cells cultured on a coverglass before or after HA'ase treatment, 150 μL of 1×10^8 cells per milliliter of erythrocyte suspension was placed on a slide with spacers. The coverglass with cells were inverted over the erythrocyte suspension, and the chamber was sealed using a soft wax and inverted again. The chamber was placed on the microscope, and the red blood cells were allowed to settle for 10 min before observation using an inverted microscope.

PCM Effect on AuNP Cellular Uptake by MG-63 Cells. To investigate the effect of PCM on AuNP cellular uptake, MG-63 cells were plated on a cleaned coverglass at a density of 1×10^4 cells/mL and cultured in a plastic cell culture dish. After culturing for 30 h, the normal MG-63 cells were in their exponential growth stage with a thick PCM. To obtain control cells with a thin PCM, the normal cells were treated with 0.1 U/mL of HA'ase at 37 °C for 60 min and then washed with PBS. Two hundred microliters of 25 pM AuNPs solution was added into either the normal or HA'ase-treated cell sample containing 800 μL of cell culture medium, and the cells were coincubated for various amounts of time. The cells were then fixed with 4% paraformaldehyde for 10 min and washed with PBS for optical imaging. To disrupt the PCM and release AuNPs trapped by the thick PCM of normal MG-63 cells, the cells could be subjected to HA'ase treatment, trypsinization, or extended fixation plus excess washing.

PCM Effect on AuNP Cellular Uptake by HeLa Cells. HeLa cells were plated on a coverglass in a plastic cell culture dish at a density of 1×10^3 cells/mL. The cells obtained after being cultured under regular conditions for 80 h are denoted as the control cells. The cells with a thinner PCM were obtained by treating the control cells with 0.1 U/mL HA'ase for 60 min. To obtain HeLa cells with an enhanced PCM, freshly prepared cell medium containing 25 $\mu\text{g}/\text{mL}$ ascorbic acid (AA) was used to replace the old cell culture medium three times after the cells were cultured for 24, 48, and 72 h,

respectively. For each type of HeLa cells, 200 μL of 25 pM AuNP solution was added into the sample containing 800 μL of cell medium and coincubated for 1 h. The cells were then fixed with 4% paraformaldehyde and washed with PBS before dark field imaging.

Imaging and Data Analysis. Dark field microscopy (DFM) was performed on an upright optical microscope Nikon 80i (Japan). White light from the halogen lamp was focused onto the sample obliquely via an oil immersion dark field condenser (NA 1.43-1.20). Scattered light from the NPs was collected using a 60 \times objective and then captured using a color CCD camera (DP72, Olympus). Laser scanning confocal microscopy (LSCM) was performed using an Olympus FV1000 microscope equipped with multiple laser lines. FM 1-43 fluorescence images and AuNP scattering LSCM images were collected simultaneously using a 60 \times objective, two separate channels with 488 nm ex/530 nm em and 635 nm ex/635 nm em, respectively, and a 120- μm pinhole. All the DFM and LSCM images were processed using ImageJ.

Quantification of AuNP Cellular Uptake Using ICP-AES. To measure the number of AuNPs entering the cells using inductively coupled plasma atomic emission spectroscopy (ICP-AES),²⁵ MG-63 cells were plated at a density of 1×10^4 cells/mL and cultured for 32 h. Then, the media of normal and HA'ase-treated MG-63 cells were replaced with fresh media containing 5 pM AuNPs. After 4 h incubation, the cells were washed with PBS three times, detached from the Petri dish using trypsin-EDTA, collected, counted, treated with nitric acid at 120 °C for 2 h, and kept at 70 °C overnight to ensure all AuNPs were dissolved completely. The concentration of Au was measured using ICP-AES, and the average number of AuNPs internalized by one cell was determined according to the size of the Au nanosphere and the atomic weight of gold. The experiment was repeated three times to obtain the mean value and the standard deviation.

■ ASSOCIATED CONTENT

📄 Supporting Information

Table, additional figures, and and avi files as mentioned in the main text. This material is available free of charge via the Internet at <http://pubs.acs.org>.

■ AUTHOR INFORMATION

Corresponding Author

yanhe2021@gmail.com

Notes

The authors declare no competing financial interest.

■ ACKNOWLEDGMENTS

This work was supported by NSFC 20975036, NSFC 91027037, Program for Cheungkong Scholars and Innovative Research Team in University, and Hunan University 985 fund.

■ REFERENCES

- (1) Rosi, N. L.; Giljohann, D. A.; Thaxton, C. S.; Lytton-Jean, A. K. R.; Han, M. S.; Mirkin, C. A. *Science* **2006**, *312*, 1027.
- (2) Thomas, M.; Klibanov, A. M. *Proc. Natl. Acad. Sci. U.S.A.* **2003**, *100*, 9138.
- (3) Ghosh, P.; Han, G.; De, M.; Kim, C. K.; Rotello, V. M. *Adv. Drug Delivery Rev.* **2008**, *60*, 1307.
- (4) Sperling, R. A.; Rivera Gil, P.; Zhang, F.; Zanella, M.; Parak, W. J. *Chem. Soc. Rev.* **2008**, *37*, 1896.
- (5) Stark, W. J. *Angew. Chem., Int. Ed.* **2011**, *50*, 1242.
- (6) Krug, H. F.; Wick, P. *Angew. Chem., Int. Ed.* **2011**, *50*, 1260.
- (7) Khlebtsov, N.; Dykman, L. *Chem. Soc. Rev.* **2011**, *40*, 1647.
- (8) Jiang, W.; Kim, B. Y. S.; Rutka, J. T.; Chan, W. C. W. *Nanotechnol.* **2008**, *3*, 145.
- (9) Mahmoudi, M.; Lynch, I.; Ejtehadi, M. R.; Monopoli, M. P.; Bombelli, F. B.; Laurent, S. *Chem. Rev.* **2011**, *111*, 5610.
- (10) Cho, E. C.; Zhang, Q.; Xia, Y. N. *Nat. Nanotechnol.* **2011**, *6*, 385.

- (11) Walkey, C. D.; Chan, W. C. W. *Chem. Soc. Rev.* **2012**, *41*, 2780.
- (12) Kim, J. A.; Aberg, C.; Salvati, A.; Dawson, K. A. *Nat. Nanotechnol.* **2012**, *7*, 62.
- (13) Canton, I.; Battaglia, G. *Chem. Soc. Rev.* **2012**, *41*, 2718.
- (14) Weinbaum, S.; Tarbell, J. M.; Damiano, E. R. *Annu. Rev. Biomed. Eng.* **2007**, *9*, 121.
- (15) Toole, B. P. *Nat. Rev. Cancer* **2004**, *4*, 528.
- (16) Vigfúsdóttir, Á.; Pasirja, C.; Thakore, P.; Schmidt, R.; Hsieh, A. *Cell. Mol. Bioeng.* **2010**, *3*, 387.
- (17) Lieleg, O.; Baumgärtel, R. M.; Bausch, A. R. *Biophys. J.* **2009**, *97*, 1569.
- (18) Suzuki, Y.; Nishida, Y.; Naruse, T.; Gemba, T.; Ishiguro, N. *J. Surg. Res.* **2009**, *152*, 148.
- (19) Nijenhuis, N.; Mizuno, D.; Spaan, J. A. E.; Schmidt, C. F. *J. R. Soc. Interface* **2012**, *9*, 1.
- (20) Philipson, L. H.; Westley, J.; Schwartz, N. B. *Biochem.* **1985**, *24*, 7899.
- (21) Hirashima, Y.; Kobayashi, H.; Suzuki, M.; Tanaka, Y.; Kanayama, N.; Fujie, M.; Nishida, T.; Takigawa, M.; Terao, T. *J. Biol. Chem.* **2001**, *276*, 13650.
- (22) Lee, G. M.; Johnstone, B.; Jacobson, K.; Caterson, B. *J. Cell Biol.* **1993**, *123*, 1899.
- (23) Dreaden, E. C.; Alkilany, A. M.; Huang, X. H.; Murphy, C. J.; El-Sayed, M. A. *Chem. Soc. Rev.* **2012**, *41*, 2740.
- (24) Xiao, L.; Wei, L.; Cheng, X.; He, Y.; Yeung, E. S. *Anal. Chem.* **2011**, *83*, 7340.
- (25) Chithrani, B. D.; Ghazani, A. A.; Chan, W. C. W. *Nano Lett.* **2006**, *6*, 662.
- (26) Palte, M. J.; Raines, R. T. *J. Am. Chem. Soc.* **2012**, *134*, 6218.
- (27) Korte, S.; Wiesinger, A.; Straeter, A. S.; Peters, W.; Oberleithner, H.; Kusche-Vihrog, K. *Pflugers Arch.* **2012**, *463*, 269.
- (28) Evanko, S. P.; Tammi, M. I.; Tammi, R. H.; Wight, T. N. *Adv. Drug Delivery Rev.* **2007**, *59*, 1351.
- (29) Zhou, R.; Xiong, B.; He, Y.; Yeung, E. *Anal. Bioanal. Chem.* **2011**, *399*, 353.
- (30) Gao, H.; Shi, W.; Freund, L. B. *Proc. Natl. Acad. Sci. U.S.A.* **2005**, *102*, 9469.
- (31) Tomas, S.; Milanesi, L. *Nature Chem.* **2010**, *2*, 1077.
- (32) Spendier, K.; Lidke, K. A.; Lidke, D. S.; Thomas, J. L. *FEBS Lett.* **2012**, *586*, 416.
- (33) Felsenfeld, D. P.; Choquet, D.; Sheetz, M. P. *Nature* **1996**, *383*, 438.
- (34) Wang, F.; Wang, Y.-C.; Dou, S.; Xiong, M.-H.; Sun, T.-M.; Wang, J. *ACS Nano* **2011**, *5*, 3679.
- (35) Walkey, C. D.; Olsen, J. B.; Guo, H.; Emili, A.; Chan, W. C. W. *J. Am. Chem. Soc.* **2012**, *134*, 2139.
- (36) Real, F. X.; Rettig, W. J.; Chesa, P. G.; Melamed, M. R.; Old, L. J.; Mendelsohn, J. *Cancer Res.* **1986**, *46*, 4726.
- (37) Chithrani, B. D.; Chan, W. C. W. *Nano Lett.* **2007**, *7*, 1542.
- (38) Leddy, H. A.; Christensen, S. E.; Guilak, F. *J. Biomech. Eng.-Trans. ASME* **2008**, *130*, 061002.
- (39) Stylianopoulos, T.; Poh, M.-Z.; Insin, N.; Bawendi, M. G.; Fukumura, D.; Munn, Lance, L.; Jain, R. K. *Biophys. J.* **2010**, *99*, 1342.
- (40) Alberts, B.; Johnson, A.; Lewis, J.; Raff, M.; Roberts, K.; Walter, P. *Molecular Biology of the Cell*, 5th ed.; Garland: New York, 2007.
- (41) Jaqaman, K.; Kuwata, H.; Touret, N.; Collins, R.; Trimble, W. S.; Danuser, G.; Grinstein, S. *Cell* **2011**, *146*, 593.
- (42) Niu, J.; Zhu, T.; Liu, Z. *Nanotechnology* **2007**, *18*, 325607.